Original Article

www.jmss.mui.ac.ir

An Optimal Partial Differential Equations-based Stopping Criterion for Medical Image Denoising

Maryam Khanian, Awat Feizi[1], Ali Davari[2]

Department of Mathematics, Khorasgan (Isfahan) Branch, Islamic Azad University, [1]Department of Biostatistics and Epidemiology, School of Health, Isfahan University of Medical Sciences, [2]Department of Mathematics, Faculty of Mathematical Sciences and Statistics, University of Isfahan, Isfahan, Iran

Submission: 18-05-2013 Accepted: 01-12-2013

ABSTRACT

Improving the quality of medical images at pre- and post-surgery operations are necessary for beginning and speeding up the recovery process. Partial differential equations-based models have become a powerful and well-known tool in different areas of image processing such as denoising, multiscale image analysis, edge detection and other fields of image processing and computer vision. In this paper, an algorithm for medical image denoising using anisotropic diffusion filter with a convenient stopping criterion is presented. In this regard, the current paper introduces two strategies: utilizing the efficient explicit method due to its advantages with presenting impressive software technique to effectively solve the anisotropic diffusion filter which is mathematically unstable, proposing an automatic stopping criterion, that takes into consideration just input image, as opposed to other stopping criteria, besides the quality of denoised image, easiness and time. Various medical images are examined to confirm the claim.

Key words: *Anisotropic diffusion filter, medical image denoising, stopping criterion*

INTRODUCTION

One of the most important fields of medical image analysis involves post acquisition like denoising, because the presence of noise in image is unavoidable. It can be caused by the image formation process, image recording and image transmission. These random distortions make problems to perform any required image processing. Even a small amount of noise is detrimental to the high accuracy analyzing, e.g., in sub-cell image analysis. Thus, removing noise is often the first step in interferograms analysis. In recent years, partial differential equations methods in image processing have been extensively used due to their good performance to improve traditional approaches. These methods cannot only remove the noise but also keep much more details without blurring or changing the location of the edges. Moreover, their scope include not only the significant problem of image denoising but also other restoration tasks such as deblurring,[1,2] blind deconvolution,[1] inpainting,[3-5] edge detection[6,7] and segmentation.[8-10] In this paper, we focus on the use of anisotropic diffusion model which has been extensively studied since it is introduced by the Perona and Malik in 1987.[11] Perona-Malik model has been considered as a useful tool for image noise removal and other areas of image processing.[12-14] However, if we decide to restore noisy images using some methods starting from an input image, which led to a set of possible filter solutions by gradually removing noise, the crucial question is when to stop filtering in order to get the optimal restoration result. The objective is quite challenging, because the stopping time has a great effect on the output result. Introducing small amount of stopping time gives more confidence to the input data, so more noise in input data is remained; whereas, most parts of the image are destroyed in the large value of stopping time.[15] On the other hand, stopping in the steady state yields an overly smooth image;[16] as a result, the time derivative acts as a regularizing parameter and a fundamental feature of abovementioned reconstruction procedure is the necessity to decide when to stop the iterations. In general, this is done by trial and error. Many studies have been conducted in the area of introducing stopping criterion. Let us briefly review previous works on the stopping criteria. Dolcetta and Ferretti defined a stopping time by finding a minimum of the performance index.[17] They need a constant that is found using an ordinary image with similar details and discontinuities. This is a rather ambiguous requirement; also they need some approximations to determine the constant. Sporring and Weickert proposed the stopping criterion based on the signal to noise ratio, the relative variance at time t and the initial image.[18] Mrazek

Address for correspondence:
Maryam Khanian, Department of Mathematics, Khorasgan (Isfahan) Branch, Islamic Azad University, Isfahan, Iran. E-mail: mar.khanian@gmail.com

and Navara extended this idea and introduced the stopping criterion by considering some assumptions to minimize the correlation of the signal and noise.[19] Other methods have been introduced to choose a stopping criterion, but most of them used statistics information[15,20] or were applied to one dimensional signal.[21] Some of the previous methods were computationally intensive.[22,23] Furthermore, the above techniques did not discuss about advancing the equation in time and the cause of iterative methods on the stopping criterion or frequency approaches. One of the working in these areas is suggested by Ilyevsky and Turkel.[16] In their stopping criterion the Perona-malik model is solved by complex and time consuming multigrid method. Here, the proposed automatic stopping criterion can satisfactory reduce the computational cost besides improving image quality and speed property in which it uses only the corrupted image content itself and does not need any additional information. The performance of proposed algorithm on medical images from the aspects of great improvement in time and denoising trough peak signal to noise ratio (PSNR) is evaluated. An outline of the paper is as follows:

In Section 2, we briefly introduce Perona-Malik model. This helps us to understand the important advantages of this model especially for medical imaging. Section 3 analyzes our new proposed stopping criterion with the important principles behind our approach. Some empirical evidences to show its efficiency based on reduced costs, PSNR analysis, and visual verification for a more systematic comparison is considered in Section 4 and the paper is concluded with a summary in Section 5.

PERONA-MALIK MODEL

The idea behind the use of the diffusion equation in image processing comes from the result of Gaussian filter in multiscale image analysis. Convolving the given image with a Gaussian filter k_σ:

$$k_\sigma(x,y) = \frac{1}{2\pi\sigma^2} exp(-\frac{x^2+y^2}{2\sigma^2}) \quad (1)$$

with standard deviation σ, is equivalent to the solution of the diffusion equation in two dimensions. Therefore, for an $N \times N$ image I the diffusion process defined as:

$$\frac{\partial}{\partial t} I(x,y,t) = \nabla^2 I(x,y,t) = \frac{\partial}{\partial x^2} I(x,y,t) + \frac{\partial}{\partial y^2} I(x,y,t) \quad (2)$$

$$0 \le x, y \le N, 0 \le I(x,y) \le L$$

Where L is the maximal gray level, $I(x, y, t)$ is the image $I(x, y)$ at time $t = 0.5\ \sigma^2$ with initial condition $I(x, y, 0) = I_0(x, y)$ and I_0 denotes the original image.

In general, this can be written as:

$$\frac{\partial}{\partial t} I(x,y,t) = div(c(x,y,t)\nabla I(x,y,t)) \quad (3)$$

$$I(x,y,0) = I_0(x,y)$$

Where $c(x, y, t)$ is the diffusion coefficient, ∇ represents the gradient operator and div denotes the divergence operator.

Perona and Malik introduced an inhomogeneous diffusivity by considering the following function for c:

$$c(x,y,t) = \frac{1}{1+\frac{|\nabla I|^2}{k^2}} \quad (4)$$

Here the parameter k is a threshold to evaluate the gradient of the image. This definition of c provides a good control for the process of denoising and edge preserving. It means that in the area with the high value of ∇I such as edges results in decreasing of c. Therefore, the problem of edge smoothing will be solved by the model of Perona-Malik. Whereas in homogeneous regions where observation of noise is more likely, ∇I is small; thus, c tends to 1; consequently, smoothing is achievable. Interestingly, there exists a relevancy between (3) and the neural dynamics of brightness perception. Cohen and Grossberg[24] presented a model of the primitive visual cortex with similar inhibition effects as in the Perona-Malik model. Furthermore, rapid decay of diffusivity c causes non-monotone flux function. This property of rapidly decreasing diffusivities are explicitly intended in the Perona-Malik method, so they offer the desirable result of blurring small fluctuations and sharpening edges in one single process.[25] The results of Perona and Malik are visually impressive; edges remains stable over a very long time. It is demonstrated[11] that edge detection based on this process clearly outperforms the linear canny edge detector. It is easily seen that many of the preceding results can be generalized to higher dimensions. This can be useful especially for medical image sequences from computed tomography (CT) or magnetic resonance imaging (MRI) images.[25]

Implementation of nonlinear diffusion filters are mostly based on finite difference methods, because they are easy to apply. Furthermore, the pixel structure of digital images provides a natural discretization of a fixed rectangular grid and they are well-suited for parallel architectures.[25] On the other hand, the Perona-Malik process is instable. However, the only observed instability result is the so-called staircasing effect. Weickert and Benhamouda[26] showed that the regularizing effect of a standard finite difference discretization is sufficient to solve instability problem and turn the Perona-Malik filter to a well-posed initial value problem. This is other

significant advantage of utilizing finite difference-based explicit scheme.

On the other hand, the problem with the explicit scheme is that due to the stability restrictions the time step must be very small, resulting in very slow convergence. As a result, in this paper a swap technique to tackle this essential difficulty of explicit method is used, so the main objectives in this article are (1) to present a fast and effective stopping criterion with low computational cost, (2) to utilize explicit algorithm due to its capabilities and as a remedy for ill-posedness problem of Perona-Malik model, (3) to provide a software technique with high ability to remove the difficulty of low convergence in the explicit scheme and decrease processing time.

In the following subsection, we introduce an effective time stopping procedure which takes the advantages of using explicit time marching algorithm, very low computationally expenses and improved quality.

NEW STOPPING CRITERION

Definitions

I. High frequencies are defined as frequencies from $\pm\frac{N}{4} to \pm\frac{N}{2}$.

II. Denote the L_2^h as a Euclidean norm of the transform of the image in the frequency domain when only high frequencies are considered (indicative of a criterion to evaluate the energy of high frequencies).

We solved Perona-Malik equation by explicit method and computed L_2^h in every iteration $(L_2^h)_i$. Then we computed high frequency relative forward difference (HFRFD) $\left(\frac{(L_2^h)_{i+4}-(L_2^h)_i}{(L_2^h)_1}\right)$ to analyze grey value fluctuations within a neighborhood of each image point, for we need information about its derivatives to understand the structure of an image.

It is known that noise is usually represented by high frequencies in the frequency domain. The converse is not true, because all high frequencies are not noise. Interestingly results arise when one probes the diagram of HFRFD. It means that at first, the rate of decreasing in L_2^h (energy of high frequencies) is fast (during the process of denoising) but after some iterations the rate of decreasing becomes slow and slower and consequently uniform (an asymptotic line) [Figure 1]. There is a region with the maximum cavity in its diagram before the asymptotic line including an important point of undulation point. This point is located close the minimum point of the curve. In this region the race of decreasing in L_2^h becomes very slow and most parts of the image is denoised; thus, in practice, more denoising after this situation is not useful and even damages the important features of image such as edges and lines.

Furthermore, with more investigation, it will be clear that the thresholds for parameter r ($r \simeq 1$ to 1.3) which is introduced in[16] as the ratio of the spectral energy of the denoised image and the blurred version of the image with no noise for a stopping criterion are located in this region; consequently, a threshold should be determined to stop denoising in this region. This threshold is selected as 0.09 by various experiments on different images with different details. Figure 1 represents L_2^h, HFRFD diagrams and the situation of r for the abdomen CT which is contaminated by a Gaussian noise of variance = 0.02. It shows the details of the proposed restoration algorithm. Thus, we will have this algorithm:

i. Solve the Perona-Malik equation and compute HFRFD as $\left(\frac{(L_2^h)_{i+4}-(L_2^h)_i}{(L_2^h)_1}\right)$.

ii. Stop when $\left(\frac{(L_2^h)_{i+4}-(L_2^h)_i}{(L_2^h)_1}\right) \le 0.09$.

We use PSNR for quantification comparing and observation manner for qualification comparing.

The PSNR is calculated as:

$$PSNR = 20\log_{10}\left(\frac{MAX}{\sqrt{MSE}}\right) \quad (5)$$

With,

$$MSE = \frac{1}{mn}\Sigma_{i=0}^{m-1}\Sigma_{j=0}^{n-1}\left|o_{ij} - R_{ij}\right| \quad (6)$$

In the equations (5) and (6) MSE is the mean square error. Where O is an original non-corrupted image, R is a restored

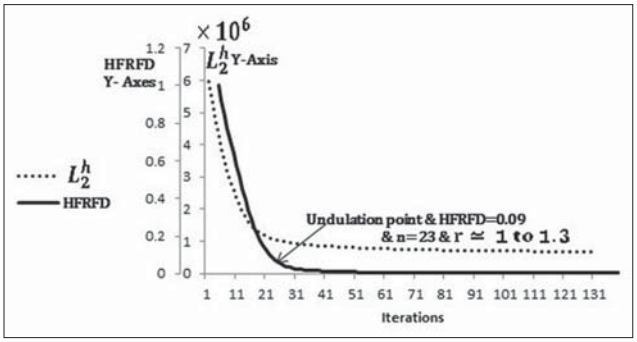

Figure 1: The L_2^h and high frequency relative forward difference reduction in every iteration for a noisy abdomen computed tomography contains a Gaussian noise of variance = 0.02 during the denoising process

image and Max is the maximum possible pixel value of the image. The advantages of proposed method from the aspects of visual and qualification criteria and processing time will be discussed in the next sections.

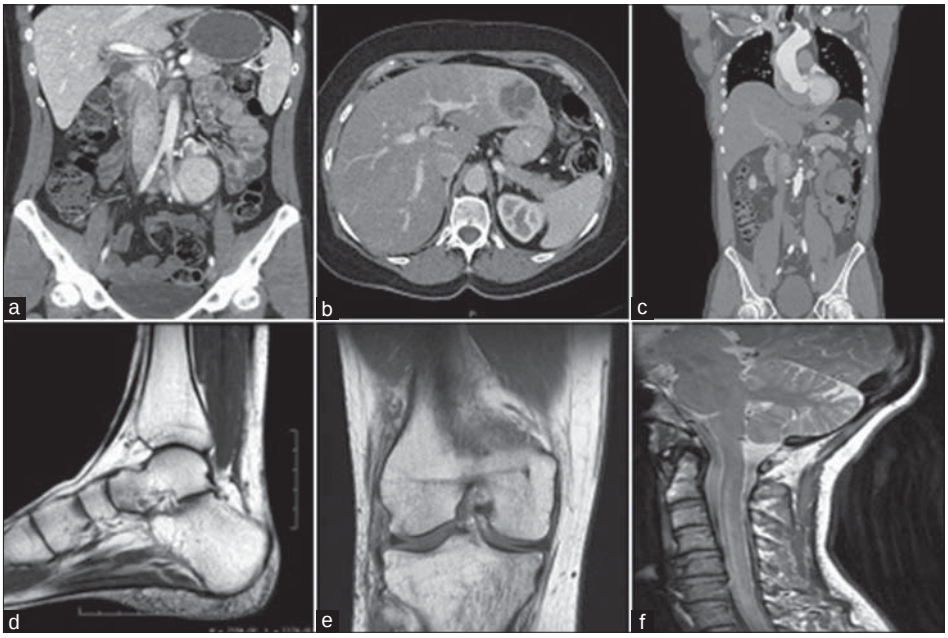

Figure 2: Tested images

Table 1: Results of implementation for proposed method and Ilyevsky algorithm using Perona-Malik model on CT images

Results of implementation for proposed algorithm (Perona-Malik model-explicit method)

Image	Variance of noise	PSNR	Time	Number of iteration
Body CT	0.02	27.3588	10.21 s	23
Body CT	0.04	27.3473	15.07 s	35
Body CT	0.08	27.3181	21.98 s	52
Pelvic CT	0.02	28.7434	9.87 s	14
Pelvic CT	0.04	28.6304	14.93 s	35
Pelvic CT	0.08	28.4805	21.98 s	52
Abdomen CT	0.02	29.2310	9.99 s	23
Abdomen CT	0.04	29.0881	14.49 s	34
Abdomen CT	0.08	28.8892	21.05 s	50

Results of implementation for Ilyevsky stopping criterion (Perona-Malik model-multigrid method)

Image	Variance of noise	PSNR	Time	Number of iteration (step 1 and step 2)
Body CT	0.02	27.2691	5639.6 s	14
Body CT	0.04	27.2095	8676.9 s	20
Body CT	0.08	27.1131	13670.2 s	31
Pelvic CT	0.02	28.7256	5633 s	14
Pelvic CT	0.04	28.6074	8723 s	20
Pelvic CT	0.08	28.4347	14295 s	32
Abdomen CT	0.02	29.2248	5674.3 s	14
Abdomen CT	0.04	29.0844	11659 s	21
Abdomen CT	0.08	28.8931	14360.4 s	32

CT – Computed tomography; PSNR – Peak signal to noise ratio

Table 2: Results of implementation for proposed method and Ilyevsky algorithm using Perona-Malik model on MRI images

Results of implementation for proposed algorithm (Perona-Malik-explicit)

Image	Variance of noise	PSNR	Time	Number of iteration
Ankle MRI	0.02	28.6108	8.84 s	20
Ankle MRI	0.04	28.5157	13.79 s	32
Ankle MRI	0.08	28.3877	22.47 s	53
Knee MRI	0.02	27.4777	9.75 s	22
Knee MRI	0.04	27.4482	14.56 s	34
Knee MRI	0.08	27.4197	22.46 s	53
Neck MRI	0.02	28.9366	10.03 s	23
Neck MRI	0.04	28.8316	15.14 s	35
Neck MRI	0.08	28.6575	22.07 s	52

Results of Implementation for Ilyevsky stopping criterion (Perona-Malik-multigrid method)

Image	Variance of noise	PSNR	Time	Number of iteration (step 1 and step 2)
Ankle MRI	0.02	28.5784	6224.5 s	14
Ankle MRI	0.04	28.4865	8674.8 s	20
Ankle MRI	0.08	28.3473	14192.3 s	31
Knee MRI	0.02	27.3957	6307.5 s	14
Knee MRI	0.04	27.3241	10116.1 s	20
Knee MRI	0.08	27.2263	14213.6 s	31
Neck MRI	0.02	28.9074	5956.9 s	14
Neck MRI	0.04	28.8173	9704.6 s	20
Neck MRI	0.08	28.6534	14578.4 s	32

MRI – Magnetic resonance imaging; PSNR – Peak signal to noise ratio

EXPERIMENTAL RESULTS

In this section, we present some examples to show the effectiveness of the proposed approach. To this aim, we used the set of images shown in Figure 2. including body CT (a), pelvic CT (b) abdomen CT (c), ankle MRI (d), knee MRI (e), and neck MRI (f) images and we added to them Gaussian noise of zero mean with different variances ($\sigma = 0.02, 0.04, 0.08$). Then the different stopping times, using proposed and Ilyevsky *et al*. methods are compared. All images are in size of 512×512; however the proposed technique can be used for higher dimensions due to its low processing time. The denoised image, in every case, is evaluated using the PSNR and processing time and optical results. The results of the measurements are shown in Table 1 and Table 2. The optical results can be seen in Figures 3-20. For each image, methods are executed by a personal computer with these characteristics:

- CPU: AMD Athlon™ 64 × 2 dual core processor 4800 + 2.50 GHz
- Memory: 2.00 G.B
- Operating system: Windows 7 (32-bit)
- Image processing software: Matlab 7.10.0.499 (R2010a).

Numerical Experiments

As it can be seen from the Table 1 that results of proposed method show much less computational cost and better PSNR is achieved for most of the images. This increase of PSNR for images with more details is higher than other cases. For example, 14 iterations of Ilyevsky method need 5633 s, and obtained PSNR is 28.7256 whereas 14 iterations of HFRFD

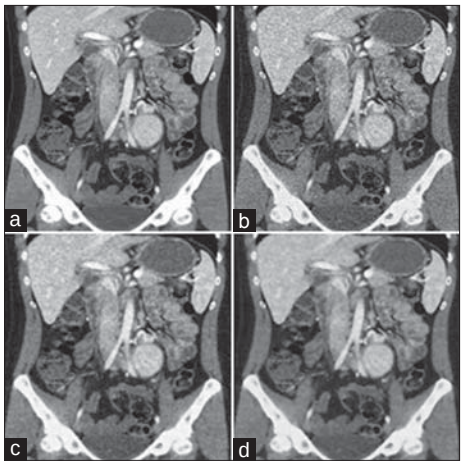

Figure 3: (a) Original image. (b) A noisy image with $\sigma = 0.02$. (c) The Ilyevsky filtering result using Perona-Malik model with $t = 5639.6$ s, peak signal to noise ratio (PSNR) = 27.2691. (d) The proposed method using Perona-Malik model with $t = 10.21$ s, PSNR = 27.3588

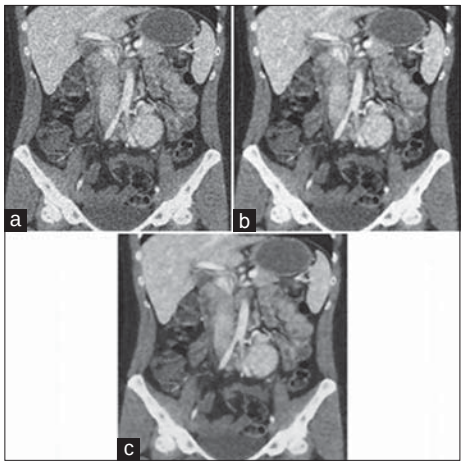

Figure 4: (a) A noisy image with $\sigma = 0.04$. (b) The Ilyevsky filtering result using Perona-Malik model with $t = 8676.9$ s, peak signal to noise ratio (PSNR) = 27.2095. (c) The proposed method using Perona-Malik model with $t = 15.07$ s, PSNR = 27.3473

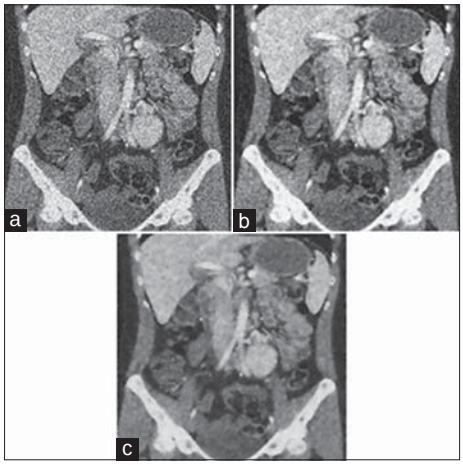

Figure 5: (a) A noisy image with $\sigma = 0.08$. (b) The Ilyevsky filtering result using Perona-Malik model with $t = 13670.2$ s, peak signal to noise ratio (PSNR) = 27.1131. (c) The proposed method using Perona-Malik model with $t = 21.98$ s, PSNR = 27.3181

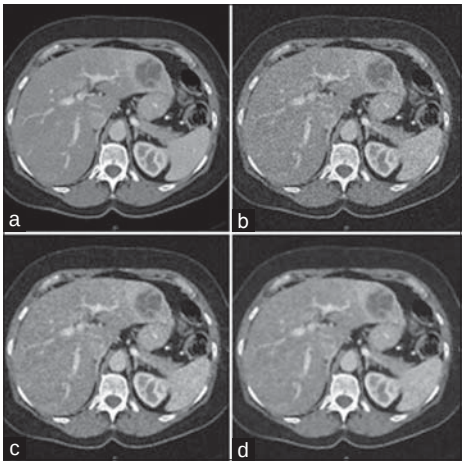

Figure 6: (a) Original image. (b) A noisy image with $\sigma = 0.02$. (c) The Ilyevsky filtering result using Perona-Malik model with $t = 5633$ s, peak signal to noise ratio (PSNR) = 28.7256. (d) The proposed method using Perona-Malik model with $t = 9.87$ s, PSNR = 28.7434

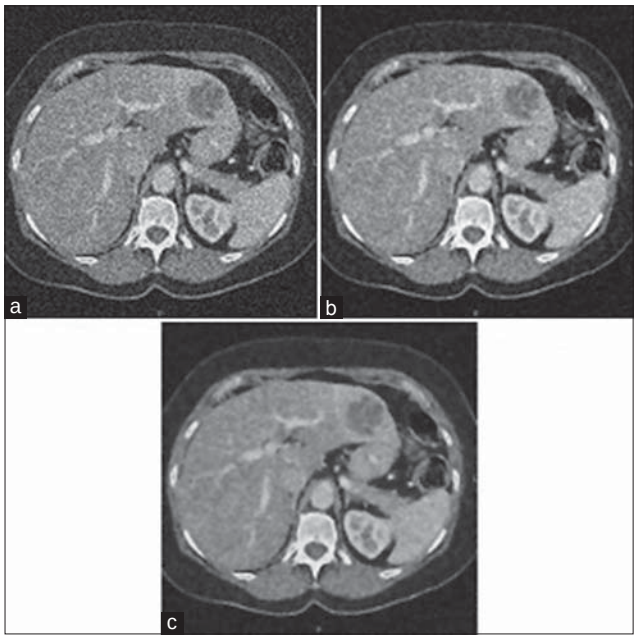

Figure 7: (a) A noisy image with σ = 0.04. (b) The Ilyevsky filtering result using Perona-Malik model with *t* = 8723 s, peak signal to noise ratio (PSNR) = 28.6074. (c) The proposed method using Perona-Malik model with *t* = 14.93 s, PSNR = 28.6304

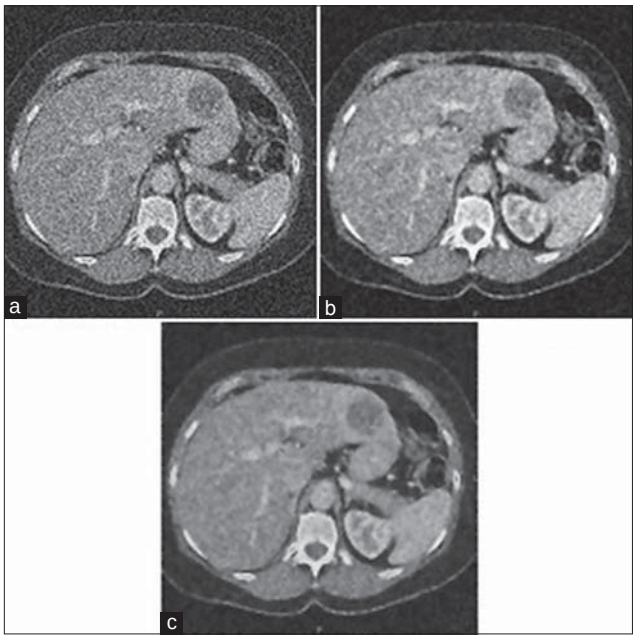

Figure 8: (a) A noisy image with σ = 0.08. (b) The Ilyevsky filtering result using Perona-Malik model with *t* = 14295 s, peak signal to noise ratio (PSNR) = 28.4347. (c) The proposed method using Perona-Malik model with *t* = 21.98 s, PSNR = 28.4805

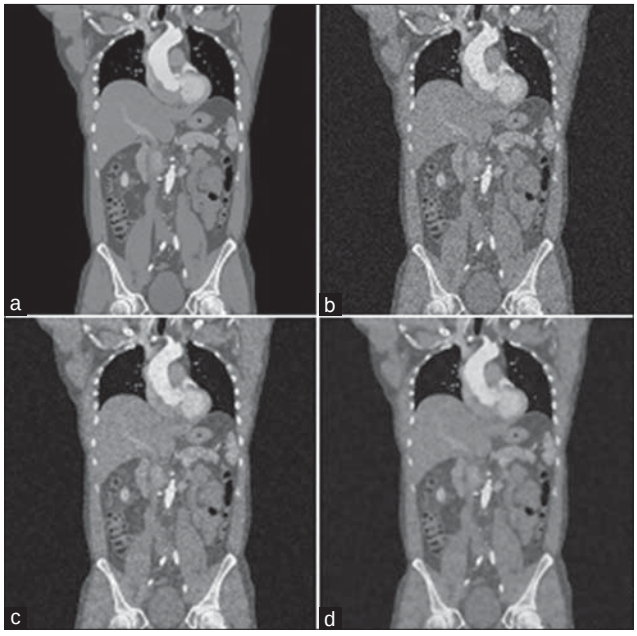

Figure 9: (a) Original image. (b) A noisy image with σ = 0.02. (c) The Ilyevsky filtering result using Perona-Malik model with *t* = 5674.3s, peak signal to noise ratio (PSNR) = 29.2248. (d) The proposed method using Perona-Malik model with *t* = 9.99 s, PSNR = 29.2310

reconstruction procedure need 9.87 s, and obtained PSNR is 28.7434 for a noisy version of Pelvic CT image with σ = 0.02. Moreover, for the body CT image with σ = 0.08, 31 iterations of the multigrid algorithm and 52 iterations of proposed technique produce restored images with PSNR = 27.1131 in 13670.2 s and PSNR = 27.3181 in 21.98

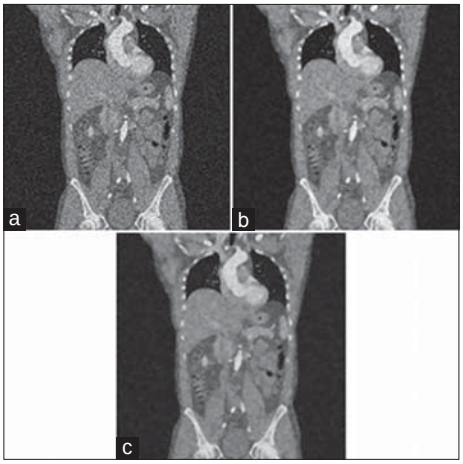

Figure 10: (a) A noisy image with σ = 0.04. (b) The Ilyevsky filtering result using Perona-Malik model with *t* = 11659 s, peak signal to noise ratio (PSNR) = 29.0844. (c) The proposed method using Perona-Malik model with *t* = 14.49 s, PSNR = 29.0881

s, respectively and finally 20 iterations of Ilyevsky method is executed in 8676.9 s, and PSNR is 27.2095 but 35 iterations of proposed procedure need 15.07 s, with PSNR = 27.3474 for the Body CT image which Gaussian noise with σ =0.02 is added to it.

It should be noted that HFRFD approach gives visually better results than those of the denoised images carried out by multigrid scheme which they seem blocky. As shown in Table 1, the proposed technique takes in general more iteration to reach its best restored image.

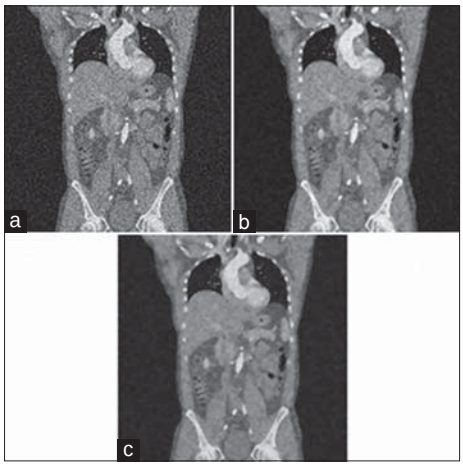

Figure 11: (a) A noisy image with σ = 0.08. (b) The Ilyevsky filtering result using Perona-Malik model with t = 14360.4 s, peak signal to noise ratio (PSNR) = 28.8931. (c) The proposed method using Perona-Malik model with t = 21.05 s, PSNR = 28.8892

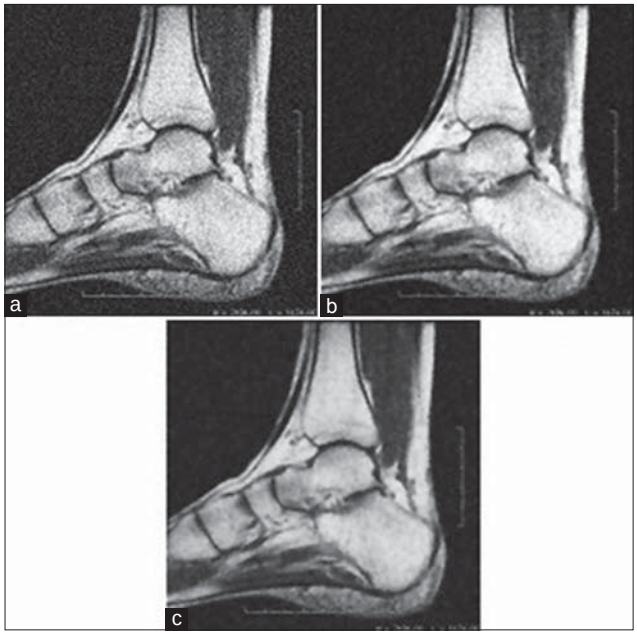

Figure 13: (a) A noisy image with σ = 0.04. (b) The Ilyevsky filtering result using Perona-Malik model with t = 8674.8 s, peak signal to noise ratio (PSNR) = 28.4865. (c) The proposed method using Perona-Malik model with t = 13.79 s, PSNR = 28.5157

However, this observation does not imply that it makes the denoising process slow down because we use swap technique. It is safe to say that the proposed algorithm does speed up the restoration procedure but runs more steps to continuously improve image quality in higher levels.

Table 2 shows PSNRs and processing time of restored images by applying two different mentioned denoising mechanisms on MRI images. It is appeared from the Table 2 that proposed algorithm shows great improvement in

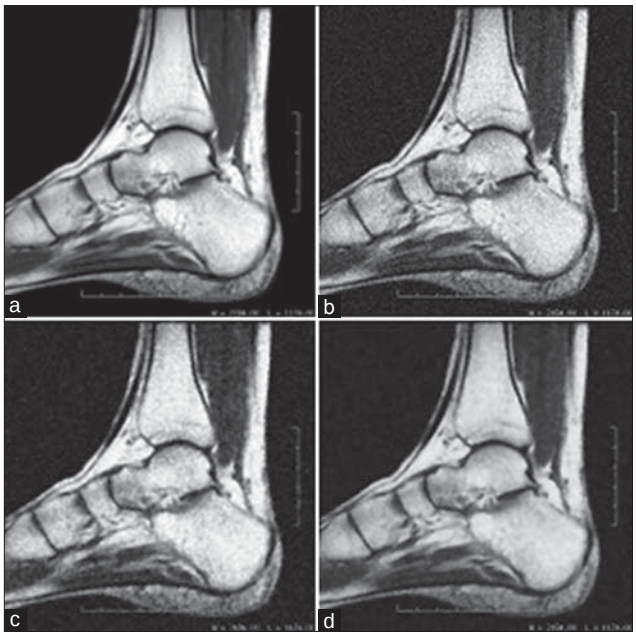

Figure 12: (a) Original image. (b) A noisy image with σ = 0.02. (c) The Ilyevsky filtering result using Perona-Malik model with t = 6224.5 s, peak signal to noise ratio (PSNR) = 28.5784. (d) The proposed method using Perona-Malik model with t = 8.84 s, PSNR = 28.6108

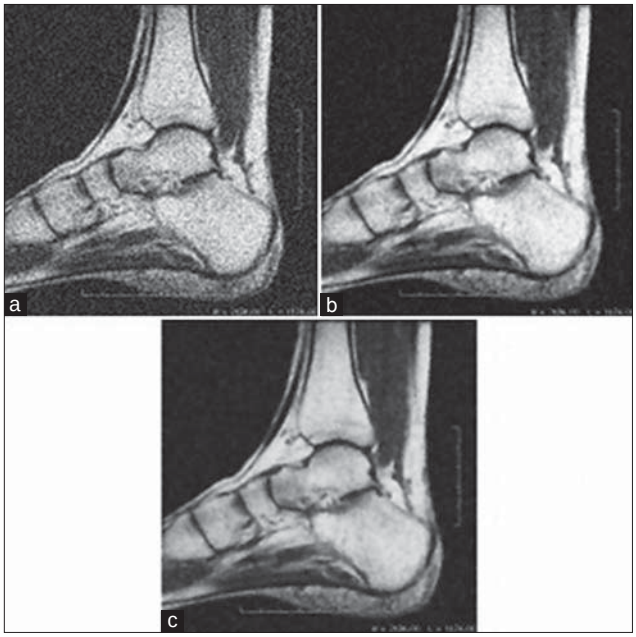

Figure 14: (a) A noisy image with σ = 0.08. (b) The Ilyevsky filtering result using Perona-Malik model with t = 14192.3 s, peak signal to noise ratio (PSNR) = 28.3473. (c) The proposed method using Perona-Malik model with t = 22.47 s, PSNR = 28.3877

computational efficiency and gains better PSNRs compared with another method for all MRI images. To illustrate, Knee MRI image with variance of 0.02 is restored by proposed strategy in t = 9.75 s with PSNR = 27.4777 and using Ilyevsky technique in t = 6307.5 s with PSNR = 27.3957.

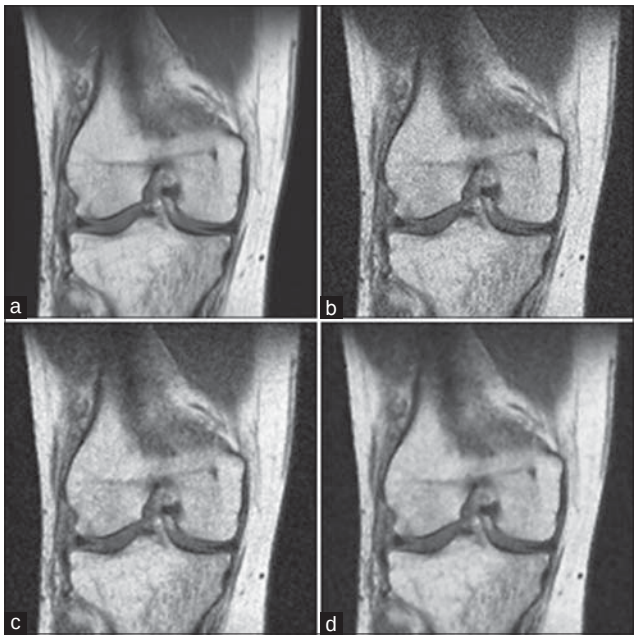

Figure 15: (a) Original image. (b) A noisy image with σ = 0.02. (c) The Ilyevsky filtering result using Perona-Malik model with t = 6307.5 s, peak signal to noise ratio (PSNR) = 27.3957. (d) The proposed method using Perona-Malik model with t = 9.75 s, PSNR = 27.4777

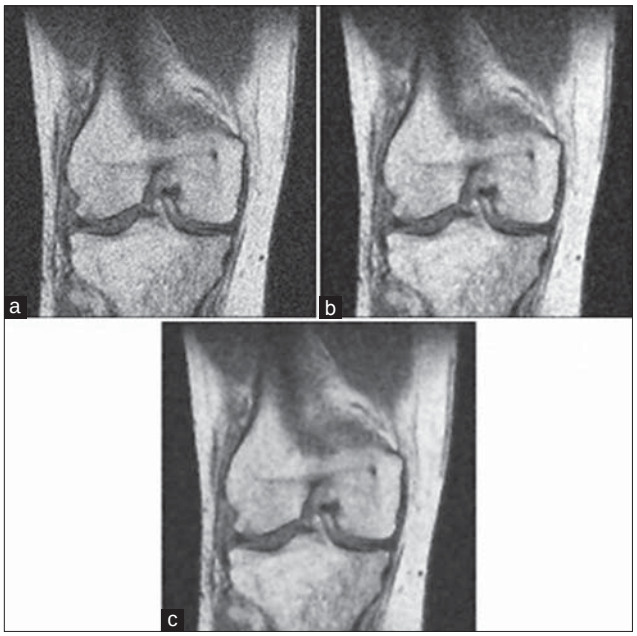

Figure 16: (a) A noisy image with σ = 0.04. (b) The Ilyevsky filtering result using Perona-Malik model with t = 10116.1 s, peak signal to noise ratio (PSNR) = 27.3241. (c) The proposed method using Perona-Malik model with t = 14.56 s, PSNR = 27.4482

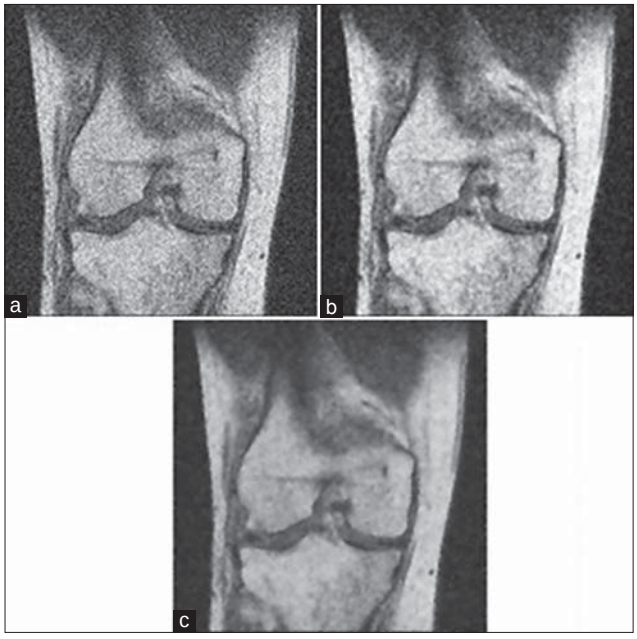

Figure 17: (a) A noisy image with σ = 0.08. (b) The Ilyevsky filtering result using Perona-Malik model with t = 14213.6 s, peak signal to noise ratio (PSNR) = 27.2263.(c) The proposed method using Perona-Malik model with t = 22.46 s, PSNR = 27.4197

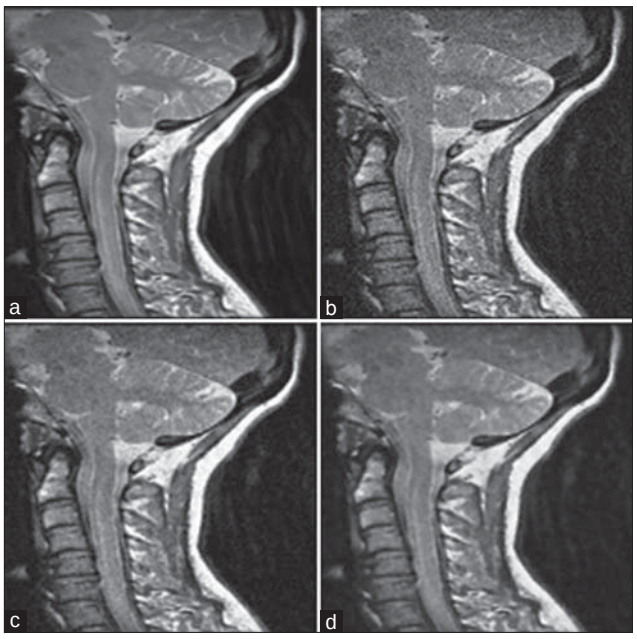

Figure 18: (a) Original image. (b) A noisy image with σ = 0.02. (c) The Ilyevsky filtering result using Perona-Malik model with t = 5956.9 s, peak signal to noise ratio (PSNR) = 28.9074. (d) The proposed method using Perona-Malik model with t = 10.03s, PSNR = 28.9366

Representing the Gradient

Following, the Sobel gradient of images, which is a popular edge detection method, yielding by our method will be presented for better analyzing a tradeoff between edge preserving and denoising. The Sobel operator is used in image processing based on an edge detection algorithm. It is a discrete differentiation operator which computes an approximation of the gradient of the image. It is based on the convolving of the image with the separable and integer valued filter in the horizontal and vertical directions. The filter is an approximation of a Gaussian

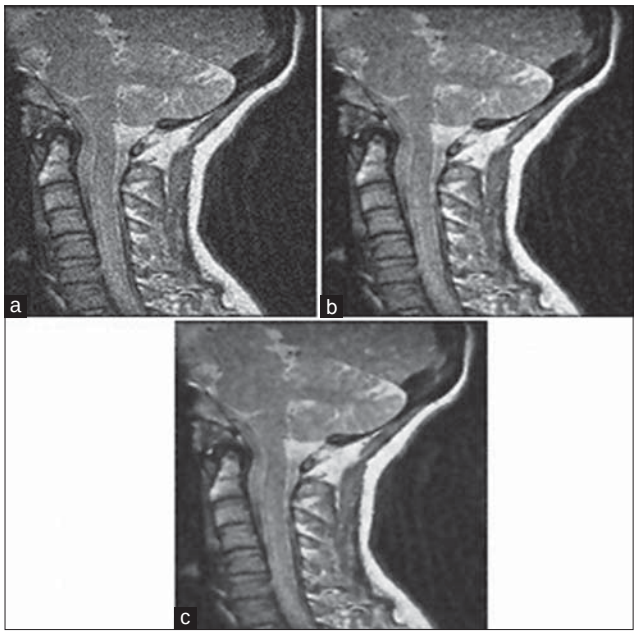

Figure 19: (a) A noisy image with σ = 0.04. (b) The Ilyevsky filtering result using Perona-Malik model with t = 9704.6 s, peak signal to noise ratio (PSNR) = 28.8173. (c) The proposed method using Perona-Malik model with t = 15.14 s, PSNR = 28.8316

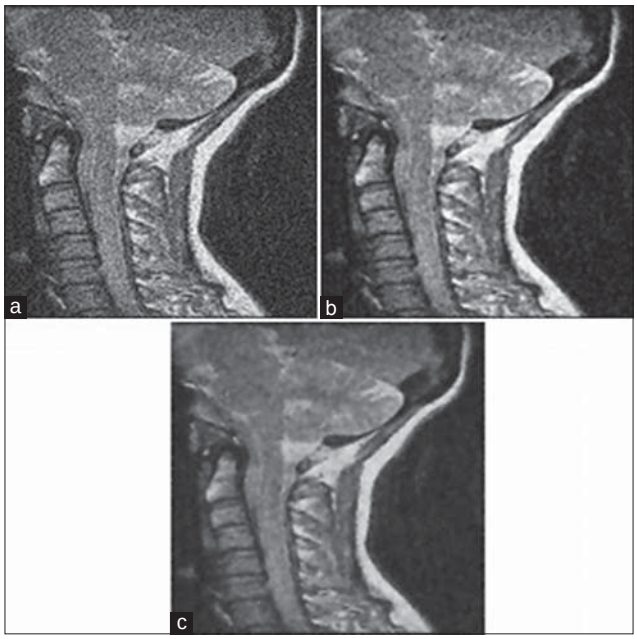

Figure 20: (a) A noisy image with σ = 0.08. (b) The Ilyevsky filtering result using Perona-Malik model with t = 14578.4 s, peak signal to noise ratio (PSNR) = 28.6534. (c) The proposed method using Perona-Malik model with t = 22.07s, PSNR = 28.6575

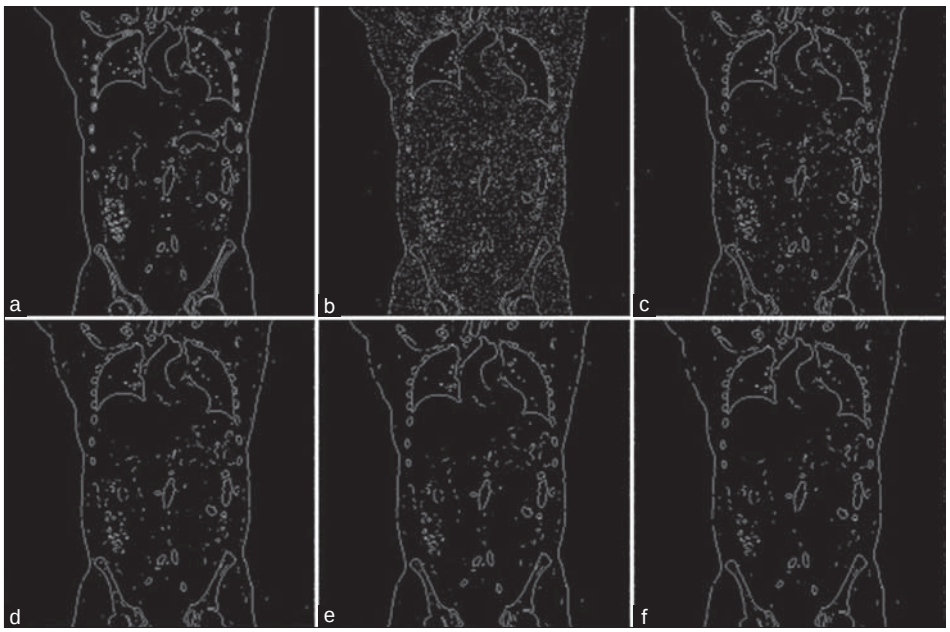

Figure 21: (a) Sobel gradient of the original image. (b) Sobel gradient of noisy image with σ = 0.02. (c) Sobel gradient of the proposed filtering result with high frequency relative forward difference (HFRFD) = 0.1. (d) Sobel gradient of the proposed filtering result with HFRFD = 0.09. (e) Sobel gradient of the proposed filtering result with HFRFD = 0.06. (f) Sobel gradient of the proposed filtering result with HFRFD = 0.03

which is the only filter that does not introduce artifacts. Each direction of Sobel filter is applied to an image. Then two new images are created. One image shows the vertical response and the other shows the horizontal response. Afterwards, two images are combined into a single image. The purpose is to determine the existence and location of edges in an image. The results of Sobel gradient images are shown in Figures 21-23. It can be seen that the difference in denoising for HFRFD = 0.09 and HFRFD = 0.1 is visible, whereas the amount of denoising with compared to degraded edges after HFRFD = 0.09 is not remarkable. This is the reason for very slow decreasing in energy of high frequencies of denoised image after HFRFD = 0.09 as shown in Figure 1.

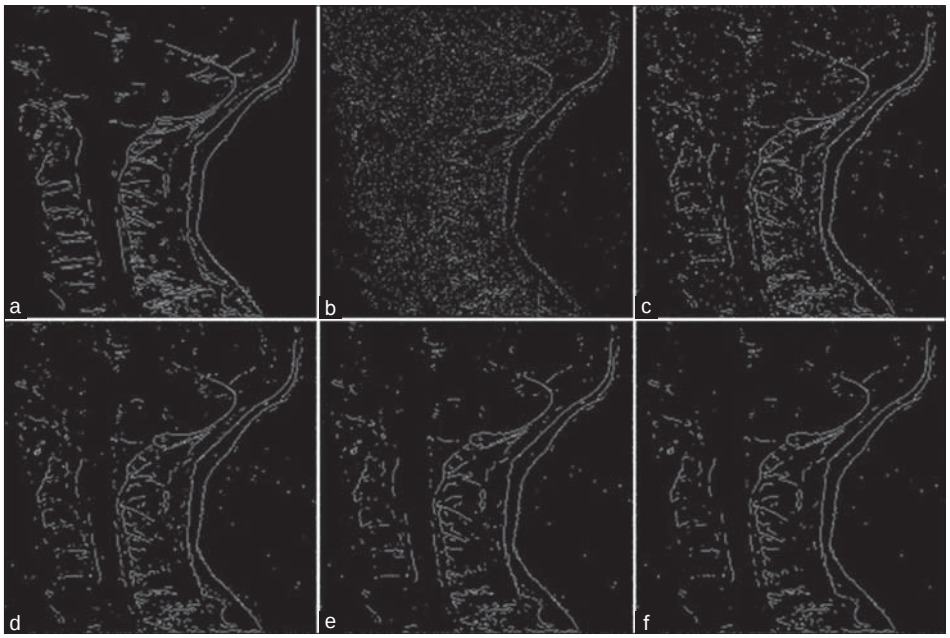

Figure 22: (a) Sobel gradient of the original image. (b) Sobel gradient of noisy image with σ = 0.04. (c) Sobel gradient of the proposed filtering result with high frequency relative forward difference (HFRFD) = 0.1. (d) Sobel gradient of the proposed filtering result with HFRFD = 0.09. (e) Sobel gradient of the proposed filtering result with HFRFD = 0.06. (f) Sobel gradient of the proposed filtering result with HFRFD = 0.03

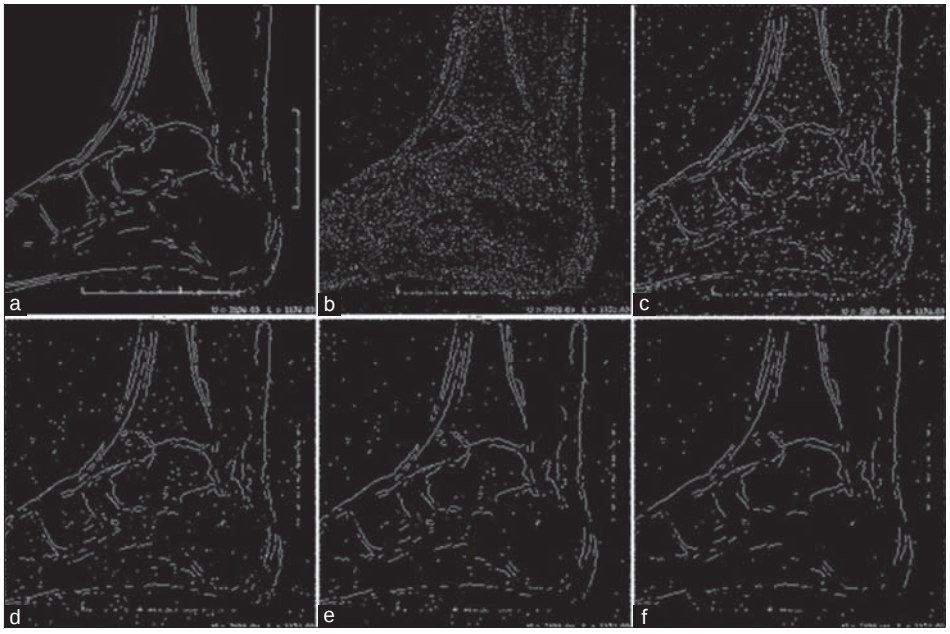

Figure 23: (a) Sobel gradient of the original image. (b) Sobel gradient of noisy image with σ = 0.08. (c) Sobel gradient of the proposed filtering result with high frequency relative forward difference (HFRFD) = 0.1. (d) Sobel gradient of the proposed filtering result with HFRFD = 0.09. (e) Sobel gradient of the proposed filtering result with HFRFD = 0.06. (f) Sobel gradient of the proposed filtering result with HFRFD = 0.03

DISCUSSION AND CONCLUSION

In the field of image processing and analysis, the problem of image denoising forms a significant preliminary step of image restoration. A major concern in image denoising models is to preserve important features such as edges and lines which are easily detected by the human visually system while denoising process. Perona-Malik model as anisotropic diffusion filter aims at degrading noise without removing fundamental parts of the image. This filter has become a valuable tool for many areas of image processing. However, this filter performs successfully as long as some important points are considered. A main feature of anisotropic diffusion procedure is presenting

an easy solving method due to its nonlinearity property in addition to removing its ill-posedness problem. The other important point is introducing the stopping time with low computational cost as a regularizing parameter which forms the quality of output image. Finally, using effective and swift software technique to handle processing time when one uses this filter is significant subject that cannot be neglected. Here, we used explicit method for addressing the ill-posedness problem of Perona-Malik model besides its other mentioned advantages.[25] Furthermore, an automatic stopping criterion is proposed that takes into consideration the quality of denoised images and uses only the content of noisy images in terms of its high frequency energies. Moreover, in order to further improvement in denoising procedure, a software technique with high capability to tackle the difficulty of low convergence in explicit scheme and processing time is introduced. We verified effectiveness of the proposed denoising strategy using several images with different levels of noise and Sobel gradient images. The results of the measurements which are shown in the Section 4 indicated that the proposed method achieved better results regarding the quality measure of denoising, visual verification, preserving important features and time.

REFERENCES

1. Weickert J. Applications of nonlinear diffusion in image processing and computer vision. Acta Mathematica Universitatis Comenianae 2001;70:33-50.
2. Drira F, Lebourgeois F, Emptoz H. Document images restoration by a new tensor based diffusion process, application to the recognition of old printed documents. In: Proc. 10th International Conference on Document Analysis and Recognition. 2009. p. 321-5.
3. Tasdizen T, Whitaker RT, Burchard P, Osher S. Geometric surface smoothing via anisotropic diffusion of normal. IEEE Vis 2002;Vol. 4:125-32.
4. Bertalmío AM, Bertozzi L, Sapiro G, Navier-Stokes. Fluid dynamics and image and video inpainting. In: Proc. CVPR Conf. 2001. p. 355-62.
5. Bredies K, Dong Y, Hintermuller M. Spatially dependent regularization parameter selection in total generalized variation models for image restoration. Int J Comput Math 2013;90:109-123.
6. Chao SM, Tsai DM. Astronomical image restoration using an improved anisotropic diffusion. Pattern Recognit 2005;27:335-44.
7. Chao SM, Tsai DM. Anisotropic diffusion based detail preserving smoothing for image restoration. In: Proc. ICIP Conf. 2010. p. 4145-8.
8. Luo HG, Zhu LM, Ding H. Coupled anisotropic diffusion for image selective smoothing. Signal Processing 2006;86:1728-36.
9. Masroor MA, DzulkiNi M. Segmentation of brain MR images for tumour extraction by combining kmeans clustering and Perona-Malik anisotropic diffusion model. Int J Image Process 2008;2:27-34.
10. Bansch E, Mikula K. A coarsening finite element strategy in image selective smoothing. Comput Vis Sci 1996;1:53-61.
11. Perona P, Malik J. Scalespace and edge detection using anisotropic diffusion. IEEE Trans Pattern Anal Mach Intell 1990;12:629-39.
12. Zeng W, Lu X, Tan X. A local structural adaptive partial differential equation for image denoising. Multimed Tools Appl 2013;67:1-15.
13. Khan NU, Arya KV, Pattanaik M. Edge preservation of impulse noise filtered images by improved anisotropic diffusion. Multimed Tools Appl 2013;67:1-25.
14. Nadernejad E, Sharifzadeh S, Forchhammer S. Using anisotropic diffusion equations in pixon domain for image de-noising. Signal Image Video Process 2013;7:1113-24.
15. Gilboa G, Sochen N, Zeevi YY. Estimation of optimal PDE-based denoising in the SNR sense. IEEE Trans Image Process 2006;15:2269-80.
16. Ilyevsky A, Turkel E. Stopping criteria for anisotropic PDEs in image processing. J Sci Comput 2010;45:337-47.
17. Dolcetta IC, Ferretti R. Optimal stopping time formulation of adaptive image filtering. Appl Math Optim 2001;43:245-58.
18. Sporring J, Weickert J. Information measures in scale-spaces. IEEE Trans Inf Theory 1999;45:1051-8.
19. Mrazek P, Navara M. Selection of optimal stopping time for nonlinear diffusion filtering. Int J Comput Vision 2003;52:189-203.
20. Tsiotsios C, Petrou M. On the choice of the parameters for anisotropic diffusion in image processing. Pattern Recognit 2013;46:1369-81.
21. Solo V. A fast automatic stopping criterion for anisotropic diffusion. In: Proc. ICASSP'02. 2002. p. 1661-4.
22. Solo V. Automatic stopping criterion for anisotropic diffusion. In: Proc. ICASSP'01. 2001. p. 3441-4.
23. Solo V. A sure-fired way to choose something parameters for total variation denoising. In: Proc. ICASSP99.IEEE. 1999.
24. Cohen MA, Grossberg S. Neural dynamics of brightness perception: Features, boundaries, diffusion, and resonance. Percept Psychophys 1984;36:428-56.
25. Weickert J. Anisotropic Diffusion in Image Processing. Stuttgart: Teubner; 1998.
26. Weickert J, Benhamouda B. A semidiscrete nonlinear scale-space theory and its relationto the Perona–Malik paradox. TFCV '96, Dagstuhl, Springer, Wien, in press. 1996.

How to cite this article: Khanian M, Feizi A, Davari A. An Optimal Partial Differential Equations-based Stopping Criterion for Medical Image Denoising. J Med Sign Sens 2014;4:72-83

Source of Support: Nil, **Conflict of Interest:** None declared

BIOGRAPHIES

Maryam Khanian received B.Sc. and M.Sc. degrees in applied mathematics in 2006, and 2011 respectively, and a Ph.D. scholarship from Brandenburg University of Technology, Germany, in 2013. Now she works on her thesis in the area of Photometric Stereo based on the Prospective Projection. She has worked in the area of image processing for about four years.

E-mail: mar.khanian@gmail.com

Awat Feizi obtained his B.S degree in Statistic in 2000 from Alameh Tabatabaei University (Tehran-Iran), MS.c in Biostatistics from Tarbiat Modares University (Tehran-Iran) in 2003 and Ph.D in Biostatistics from Tarbiat Modares University (Tehran-Iran) in 2008. He joint to Department of Biostatistics and Epidemiology at school of health in Isfahan University of medical sciences as an assitant professor and now is working as an Associate professor of Biostatistic at Department of Biostatistics and Epidemiology.

E-mail: awat_feiz@hlth.mui.ac.ir

Ali Davari received his Ph.D. degree in 2004 from Kharazmi University, Tehran, Iran. He spent 1.5 years as a Postdoctoral researcher at the University of Isfahan, Isfahan, Iran. He is an assistant professor in the department of mathematics at University of Isfahan, Isfahan, Iran.

E-mail: a_davari@sci.ui.ac.ir